

AXIAL INJECTION IN THE K500 SUPERCONDUCTING CYCLOTRON*

F. Marti and A. Gavalya
 NSCL, Michigan State University, East Lansing, Michigan 48824, USA

Abstract

The NSCL K500 superconducting cyclotron has been operating with an ECR ion source and an axial injection system since early 1986. This paper presents the results of the calculation, design and operation of the vertical injection line under the cyclotron, with special emphasis on the spiral inflector, central region and buncher.

The high magnetic field in the cyclotron (3 - 5 Tesla) imposes strict restrictions on the size of the inflector. The inflector has successfully reached and operated at the design voltage of 9.5 kV in a gap of 4 mm.

We discuss the bunching efficiency under different operating conditions and problems associated with debunching during the yoke traversal.

The spiral inflector central region includes features which act to electrically isolate the dees from each other.

Introduction

The K500 cyclotron has been operating with an axial injection system since March 1986. The beam, from a room temperature ECR¹, exits the source vertically down, and is transported to the basement level under the cyclotron axis. The beam transport system² forms a waist in both transverse directions after the second 90° magnet at a point 3 m below the cyclotron median plane. The phase space ellipse is approximately 100π mm mrad. A solenoid placed 2.22 m below the cyclotron median plane provides the focusing required to complement the cyclotron intense fringe field at low excitations (B_o = 3 T, B_{sol} = 0.12 T). This focusing complement is not needed at high excitations (B_o = 5 T, B_{sol} = 0).

We have reserved space for an electrostatic quadrupole between the 90° bending magnet and the solenoid, construction will begin after a thorough evaluation of the beam transport and injection systems has been completed.

The design calculations were performed using our axial injection code which integrates the nonlinear equations of motion in a magnetic field. The field off-axis is obtained as an expansion in powers of r of the axial field calculated with POISSON. The electric fields for the electrostatic quad, central region and the inflector are calculated using RELAX3D.³

For more details concerning the options considered, refer to our preliminary studies⁴. Several other laboratories are designing similar systems^{5,6} for superconducting cyclotrons.

Spiral Inflector

The major difficulty in the design of the central region for a superconducting cyclotron is the space limitation resulting from the size of the first turn orbit in the high magnetic field. The inflector and

the posts for the dees are located inside this first turn (see Fig. 1). With gaps between the dees and the RF cover for the inflector occupying most of the available space (the gaps are 1 cm with E= 100 kV/cm), the space for the inflector is limited to approximately 2.7 cm.

We have chosen a spiral inflector of the type built by Belmont and Pabot⁷ at Grenoble. The parameters that define the inflector are related by:

$$K = A / (2\rho_m) \quad (1)$$

where ρ_m is the radius of curvature of the orbit in the magnetic field and A is the vertical distance in which the beam is bent from vertical to horizontal (and inversely proportional to the electric field in the inflector). The parameter K defines the shape of the inflector. The value of ρ_m is determined by the injection energy of the ions with the smallest radius of curvature (V_{inj} = 20 kV, Q/u=0.5, ρ_m = 0.8 cm). We have selected K=1.1 trying to minimize the horizontal cross section of the inflector. Smaller values of K require larger electric fields and make the inflector

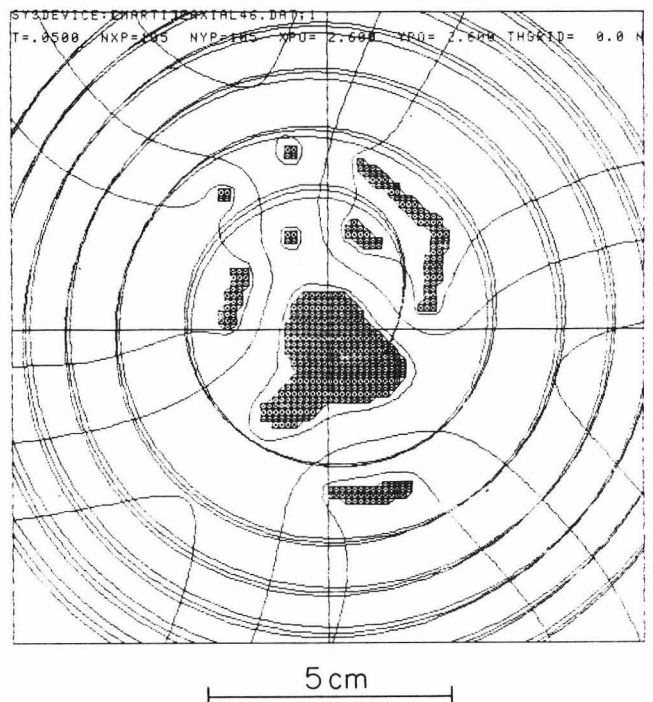


Fig. 1--Central region electrodes and equipotentials. Three orbits with starting times 240±10 RF degrees are plotted.

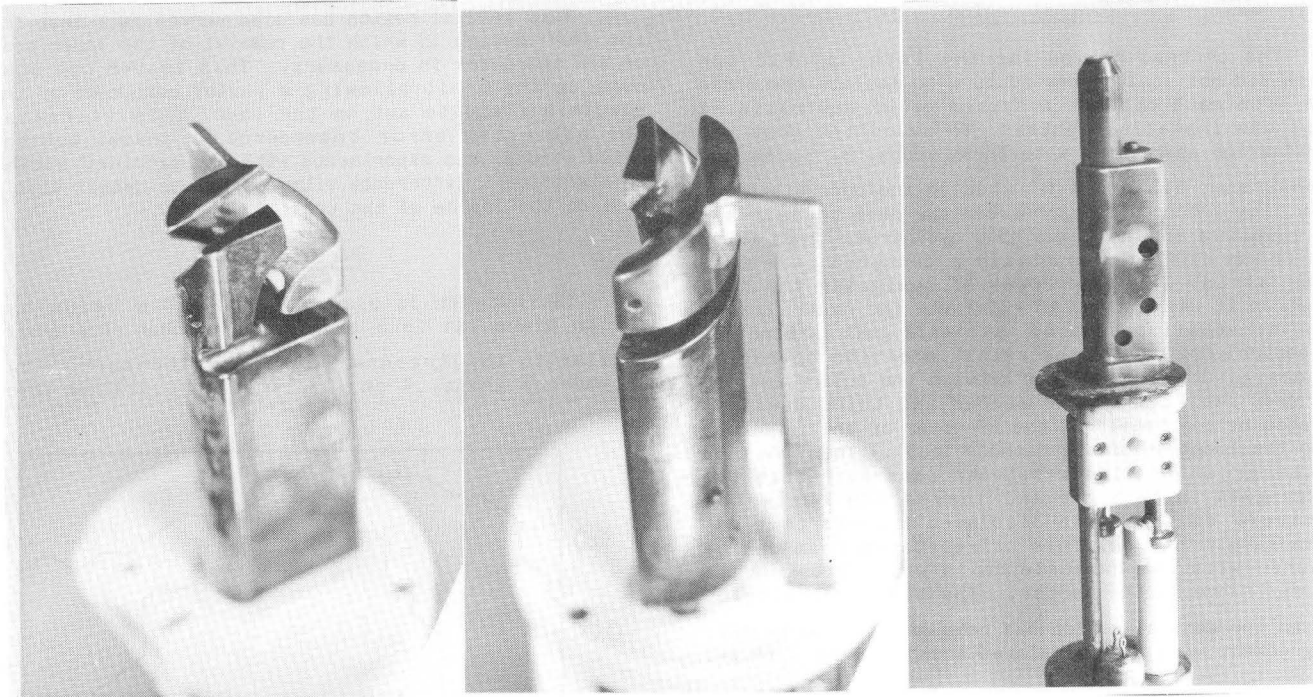


Fig. 2--Photographs of the spiral inflector, showing the electrodes, cathode lead, and RF cover. The gap is 4 mm wide, and the beam exit hole in the RF cover is 6 mm diameter. The inflector had been in operation for six months when these pictures were taken.

very small vertically and the gap between the electrodes become dominant. The gap in our inflector is 0.4 cm and the peak electric field close to 9.5 kV. It has been reached successfully. Figure 2 shows three photographs of the inflector. The electrodes and collimator (0.4 cm aperture) are molybdenum while the RF cover (seen in 2c) and high voltage leads are copper. The electrodes were fabricated by producing a molybdenum blank of the finished horizontal cross section using a wire electron discharge machine and parting the blank into two electrodes by passing a 4 mm diameter cutter along the intended beam path.

As the gap size is comparable to the beam size and we want to include the edge effect on the ion motion, the electric field is calculated by relaxation in a grid of 81x93x91, with 15 points across the gap. Figure 3 shows a plot of the equipotentials at a cross section at the entrance of the electrodes. The performance of the inflector has agreed with the calculations, and its position and voltages determined with the ion tracking program have not been changed in actual operation. We do not have indications of significant losses in the inflector.

Due to the high magnetic field in the final 50 cm of the trajectory inside the yoke hole, the ions moving off axis have a significantly longer trajectory than the ions on axis. Figure 4 shows the equal time contours in the (x, x') plane for a beam that starts at $z = -3$ m below the cyclotron. We assume $y = y' = 0$. Normally we run a grid of points in the (x, x', y, y') space and interpolate in that grid for a specific coupling or correlation. Figure 4 (top) shows the contours for $\Delta t = 2$ to 20 every 2 RF degrees (first harmonic) using the ray with $x = x' = 0$ as a reference. The bottom part of the figure shows the same contours after exiting the inflector. The shadowed area corresponds to ions that get within 3% of the gap size to the electrodes and are eliminated from the calculation.

We can find the points in the starting (x, x') plane that end within a rectangle of given size in phase space at the exit of the inflector. The top plot in Fig. 5 shows the points that exit with $|\Delta x| < 1$ mm and $|\Delta x'| < 0.1$ rad, and the inside curve with $|\Delta x| < 0.5$ mm and $|\Delta x'| < 0.05$ rad. Similar curves are shown for $|\Delta y|$ and $|\Delta y'|$ in the middle plot where x is now in the

median plane and y in the vertical plane perpendicular to the central ray. The bottom plot shows the minimum distance to the electrodes as a percent of the gap size.

The quadrupole was turned off in the previous calculations. By changing its strength and the solenoid field we can better match the cyclotron acceptance to the phase space delivered by the transport system.

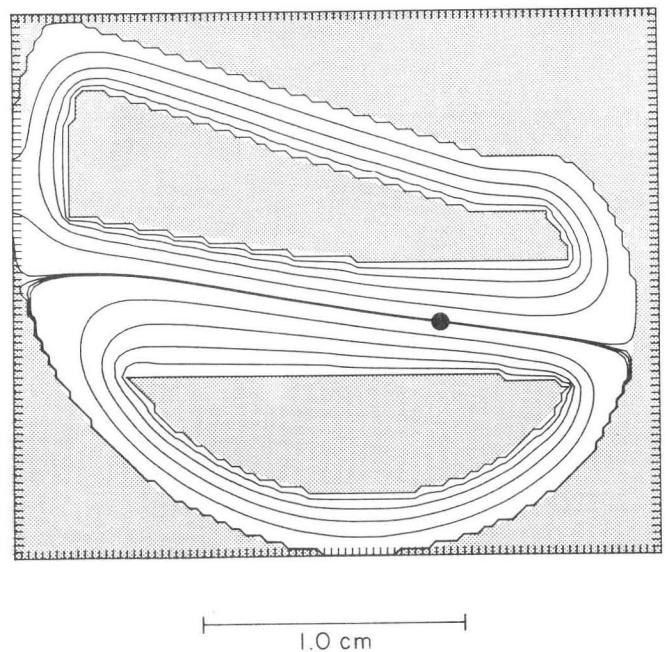


Fig. 3--Equipotentials at the entrance of the spiral inflector. The dot indicates the position of the beam.

Central region

The central region for the internal PIG ion source did not include any feature to isolate the three dees from each other. A system of RF neutralizing loops was installed instead. To avoid the cost and difficulties associated with these loops, B. Laune and B. Rogers at Texas A & M⁸ studied the possibility of installing grounded slits between the dees to decrease the coupling in the Texas K500 cyclotron. They found that it was difficult to obtain a centered beam with these slits. In the process of designing the K800 cyclotron it was decided to eliminate the neutralizing loops if at all possible. With this goal in mind the new central region for the axial injection operation was designed with a window between the puller and the next dee, see Fig. 1. The second and third dees are isolated by the "tail" of the RF cover of the inflector (also the location of the cathode lead). The insertion of the grounded window between dees decreases the energy gain in that gap and leaves the center of curvature of the orbit displaced towards that gap approximately 0.25 cm. This off-centered beam can be centered with the harmonic coils while crossing the $\nu_r=1$ resonance at the center. The beam transmission through the central region has been measured to be 12%, in agreement with the calculated acceptance of $\pm 20^\circ$ RF.

This central region has also served as a test for the K800 design in which the removal of the inner post on the third dee is necessary. This leaves one post outside the orbit allowing a radial component of the electric field to act on the ions. This increases the centering error dependence on phase, but the calculations, and experiments with the machine, showed no significant difference with a previous design with a post on the inside of the orbit.

Buncher

The buncher is placed at $z=-1.7$ m below the median plane. It is a single gap buncher of a design similar to the Argonne low energy buncher.⁹ Two molybdenum grids, 4 cm in diameter, 0.0127 cm thick

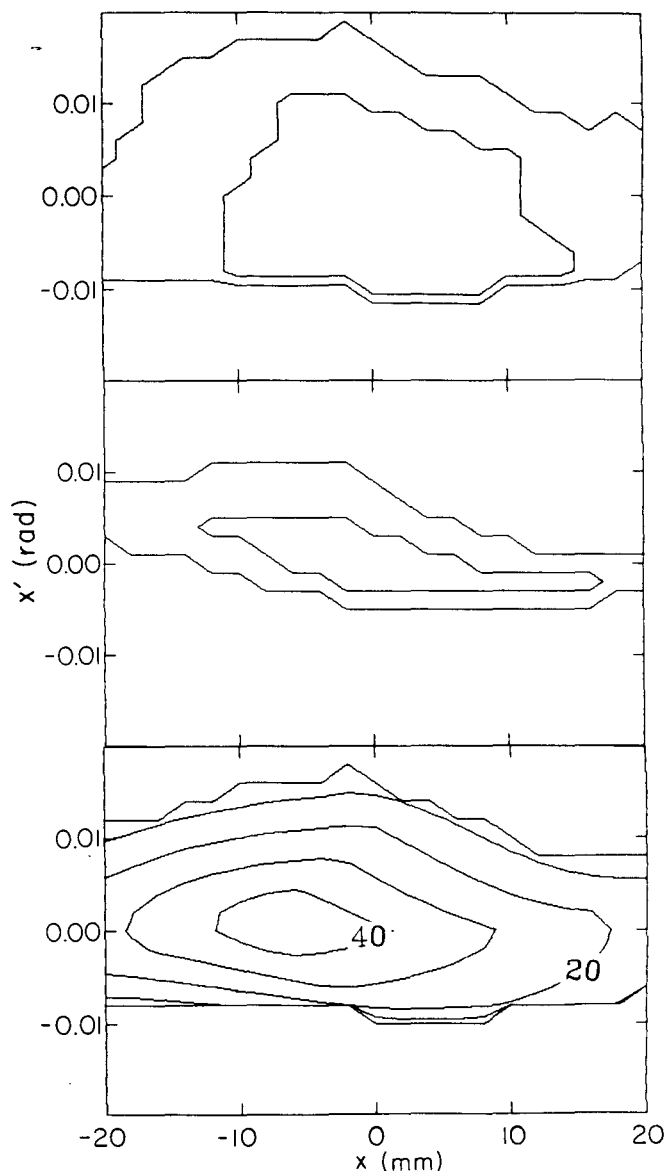
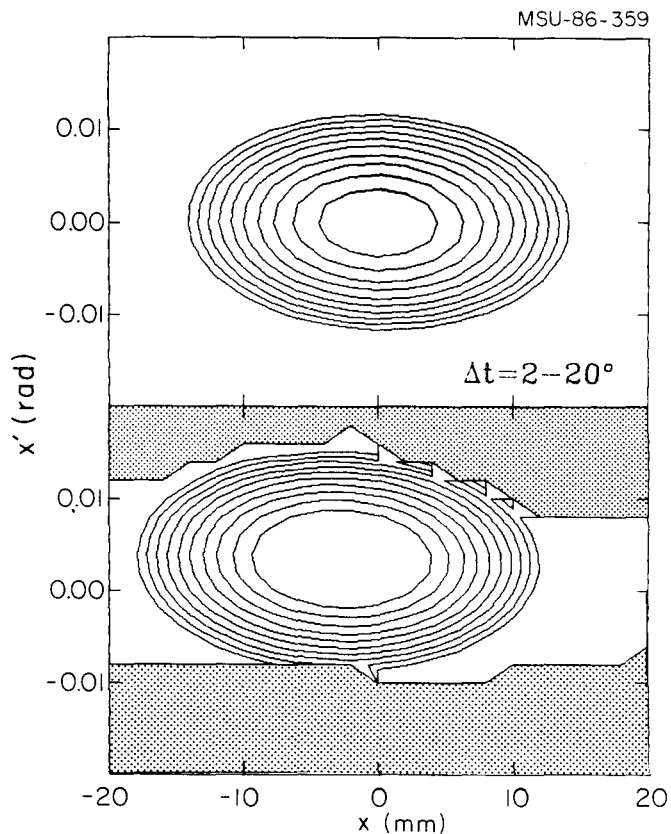


Fig. 4--The equicontours join points with equal arrival time at the inflector entrance (top) and at the inflector exit (bottom). The starting conditions (x, x') are given at a point 3 m below the cyclotron median plane. The contours for $\Delta t=2$ to 20 RF degrees (first harmonic) with respect to $x=x'=0$ are given. $Q/u=0.5$, $B_0=3.63$ T, and $y=y'=0$.

Fig. 5 At the top, starting conditions of the ions at $z=-3$ m that exit the inflector in a rectangle in phase space with $|\Delta x| < 1$ mm and $|\Delta x'| < 0.1$ rad. The inner curve corresponds to 0.5 mm and 0.05 rad. The middle plot corresponds to the (y, y') phase space. The bottom plot shows the minimum distance of approach to the electrodes as a percent of the gap distance.

with a distance of 0.152 cm between wires, are placed 0.7 cm apart. The grids are mounted in two cones that expand away from the grids. The purpose of the cones is to increase the distance over which the voltage change from ground to RF voltage is applied, and thus minimize the effect of the fringe field. Orbit tracking in the buncher electric field has shown this geometry to be effective.

One of the two grids is excited with the first harmonic of the RF voltage while the second remains grounded, or is excited with the second harmonic. The second harmonic system remains to be built.

As we showed in Fig. 4, the yoke traversal and inflector contribute greatly to the time spread of the beam at the median plane. To estimate the effect of this debunching we simulated a beam with a circular phase space in (x, x') given by:

$$x^2 + x'^2 \leq 100, \quad x \text{ in mm and } x' \text{ in mrad} \quad (2)$$

and a current density given by:

$$I = e^{-d^2}, \quad \text{where } d^2 = (x^2 + x'^2)/100. \quad (3)$$

The buncher efficiency, defined as the current captured in a $\pm 20^\circ$ phase range divided by the 360° current, is shown in Fig. 6. To make comparisons easier we have plotted the current gain in Fig. 7, defined as current with buncher on divided by current with buncher off. The gain is plotted as a function of the first harmonic grid voltage (no second harmonic). The ideal curve, no yoke or inflector effect present, is not much higher than the debunched curve for a phase acceptance of $\pm 20^\circ$, but is significantly higher in the $\pm 5^\circ$ case. The crosses indicate measurements done on the extracted beam where many tuning parameters come into play. Different beams show marked differences, with the gain reaching values above 6 in some cases.

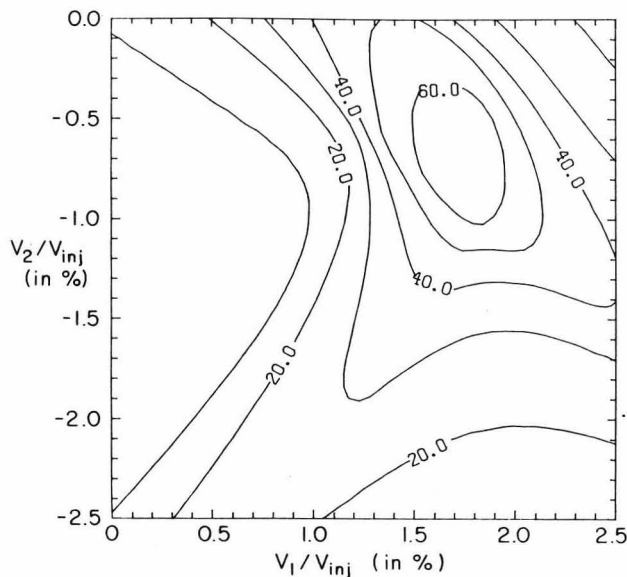


Fig. 6--Buncher efficiency (current in a $\pm 20^\circ$ interval divided by the 360° current) as a function of the first and second harmonic voltages. The time spread introduced by the yoke and inflector (Fig. 4 bottom) has been convoluted with the buncher time change. A circular beam in (x, x') space with a gaussian profile has been assumed (see text).

Current gain with first harmonic only

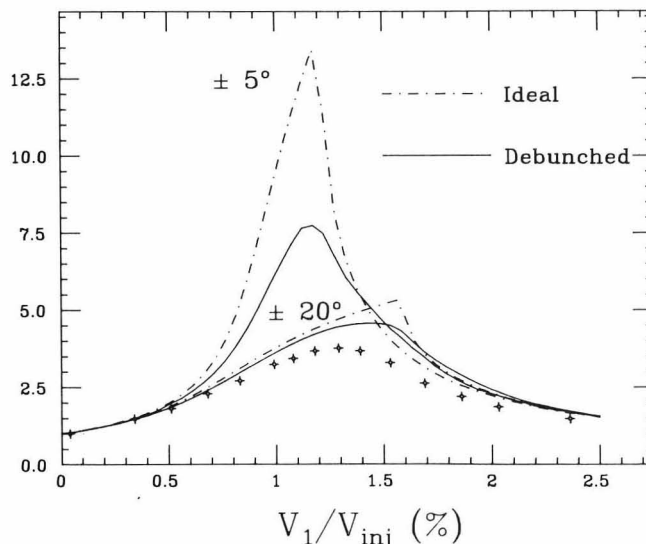


Fig. 7 Buncher gain (current with buncher on divided by current with buncher off) for a phase acceptance of ± 5 and ± 20 RF degrees, first harmonic. The solid curve simulates a beam with circular phase space in (x, x') (see text). The dashed curve is for the ideal case of no debunching produced by the yoke or inflector. The crosses are experimental data for beam current extracted from the cyclotron.

Conclusions

The operation of the ECR and the axial injection system has been very reliable and has greatly improved the overall performance of the K500 cyclotron. The agreement between the calculated and actual performance of the spiral inflector has been very good. In spite of the small size it has had a reliable operation. The overall transmission from the ECR to extracted beam is approximately 10% with the buncher on.

We would like to thank Dr. R. Pardo for sending us detailed information on the Argonne buncher.

* Work supported by NSF under Grant No. PHY-83-12245

References

1. Paper H11 by T. A. Antaya, Z. Q. Xie and J. M. Moskalik at this Conference.
2. Paper H8 by L. H. Harwood, J. A. Nolen, A. F. Zeller and S. Tanaka at this Conference.
3. H. Houtman, C. J. Kost, paper at the EPS Conf. on Computing in Acc. Design, (Berlin) 1983.
4. F. Marti, J. Griffin and V. Taivassalo, IEEE Trans. Nucl. Sc. NS-32, 2450 (1985).
G. Bellomo, D. Johnson, F. Marti and F. G. Resmini, Nucl. Inst. and Meth. 206, 19 (1983).
5. G. Bellomo, L. Serafini and F. G. Resmini, Proc. 10th Int. Conf. Cyclotrons (East Lansing) 150 (1984).
6. J. Shapira and P. Mandrillon, Proc. 10th Int. Conf. Cyclotrons (East Lansing) 332 (1984).
7. J. L. Belmont and J. L. Pabot, IEEE Trans. Nucl. Sc. NS-13, 191 (1966).
J. L. Belmont, personal communication (1984).
8. B. Laune and B. Rogers, personal communication (1984).
9. F. J. Lynch et al., Nucl. Inst. and Methods 159, 245 (1979).
R. Pardo, personal communication (1985).